Universiteit Antwerpen

This item is the archived peer-reviewed author-version of:

Accelerated molecular dynamics simulation of large systems with parallel collective variable-driven hyperdynamics

Reference:
Fukuhara Satoru, Bal Kristof, Neyts Erik, Shibuta Yasushi.- Accelerated molecular dynamics simulation of large systems with parallel collective variable-driven hyperdynamics
Computational materials science - ISSN 0927-0256 - 177(2020), 109581
Full text (Publisher's DOI): https://doi.org/10.1016/J.COMMATSCI.2020.109581
To cite this reference: https://hdl.handle.net/10067/1667730151162165141

uantwerpen.be
Institutional repository IRUA

Accelerated molecular dynamics simulation of large systems with parallel collective variable-driven hyperdynamics

Satoru Fukuhara[1]*, Kristof M. Bal[2], Erik C. Neyts[2] and Yasushi Shibuta[1]

[1]*Department of Materials Engineering, The University of Tokyo*

7-3-1 Hongo, Bunkyo-ku, Tokyo 113-8656, Japan

[2]*Department of Chemistry, University of Antwerp*

Universiteitsplein 1, 2610 Wilrijk, Antwerp, Belgium

The limitation in time and length scale is a major issue of molecular dynamics (MD) simulation. Although several methods have been developed to extend the MD time scale, their performance usually deteriorates with increasing system size. Therefore, an acceleration method which is applicable to large systems is required to bridge the gap between the MD simulations and target phenomena. In this study, an accelerated MD method for large system is developed based on the collective variable-driven hyperdynamics (CVHD) method [K.M. Bal and E.C. Neyts, 2015]. The key idea is to run CVHD in parallel with rate control and accelerate multiple possible events simultaneously. Using this novel method, carbon diffusion in bcc-iron bicrystal with grain boundary is examined as an application for practical materials. Carbon atoms reaching at the grain boundary are trapped whereas carbon atoms in the bulk region diffuse randomly, and both dynamic regimes can be simultaneously accelerated with the parallel CVHD technique.

Keywords: Accelerated molecular dynamics; Collective variables; Hyperdynamics; Diffusion;

*Corresponding Author. Tel.: +81-3-5841-7119, E-mail: fukuhara@mse.mm.t.u-tokyo.ac.jp (S. Fukuhara)

1. Introduction

The recent progress in high-performance computing is expanding the range of application of molecular dynamics (MD) simulations [1]. The length scale of MD simulations for practical metallic materials now reaches up to micrometers, or up to 10 billion atoms [2,3]. That is, the system size of large-scale MD simulations now overlaps that of mesoscale simulations such as phase-field (PF) simulation. This overlap enables the direct mapping of the information from atomistic to continuum simulations [4]. On the other hand, it is not straightforward to expand the time scale of MD simulations although the time scales of kinetic and dynamic phenomena in solid materials are usually much longer than that of the MD simulation. For example, the diffusion coefficient of carbon in low-carbon steel at 1000 °C is of the order of 10^{-6} to 10^{-7} cm^2/s [5]. Therefore, it is indispensable to establish a time-acceleration technique for MD simulation.

Already in the 1990s, Voter proposed the hyperdynamics method to accelerate MD simulation of infrequent events in solids [6]. The basic idea of hyperdynamics is to push the system out of the energetic local minima, i.e. the potential energy basin, by adding additional bias to the potential energy surface. This method is quite powerful when an appropriate bias potential can be set for the system. One problem of hyperdynamics (and many other acceleration methods) is poor scaling with system size. One approach to overcome this problem is accelerating reactions in parallel by spatial decomposition of the system [7]. In case of hyperdynamics, local hyperdynamics [8] was proposed. This method decomposes the system into local domains and uses a different bias potential for each subdomain, which is not directly affected by events occurring in other domains.

Another problem in hyperdynamics is that constructing a practical and efficient functional form of the bias potential is not straightforward in a complex system. That is, the precise shape of an optimal bias potential for each possible process is difficult to define in

advance. This is less of an issue in the metadynamics method, which also uses a bias potential to escape local energy minima [9]. Metadynamics only requires the definition of a generalized reaction coordinate referred to as a collective variable (CV). Based on the CV, the bias potential is dynamically constructed on the fly unlike hyperdynamics, in which the additional bias potential function is defined in advance. However, conventional metadynamics is constrained in configuration space by the choice of CV: it is therefore not suited for exploration of the dynamical time evolution of the system, but typically used to study the free energy surface (FES) of a single process described by the CV. Moreover, various related techniques such as adaptive boost MD [10] and diffusive molecular dynamics (DMD) [11] have been proposed to accelerate the time scale of the MD simulation.

Recently, Bal and Neyts proposed collective variable-driven hyperdynamics (CVHD) [12], in which strengths of metadynamics are implemented into hyperdynamics. Specifically, explorative unconstrained dynamics can be captured in a scheme of metadynamics by resetting bias potential and CV after each transition event. So far, CVHD has been successfully applied for various types of reactions such as fuel combustion [13, 14], graphite etching [15, 16] and catalytic reactions [17]. This way, different types of processes can be accelerated in a single CVHD simulation, during which optimal bias potentials are generated on the fly for each event. However, like other hyperdynamics methods, CVHD also suffers from poor scaling with the system size. For example, when the present CVHD method is used to accelerated two reactions occurring simultaneously in different parts of the system, the acceleration rate decreases in principle by a factor of 2 compared with the case of one reaction.

In order to overcome this problem, a parallel CVHD method is newly developed in this study, in which multiple independent reactions are independently accelerated at a target acceleration rate. The resulting parallel CVHD method retains the flexible bias of the standard CVHD method,

while extending its applicability to much larger systems and problems relevant to materials science. Then, using this method, diffusion of multiple carbon atoms in a bcc-iron bicrystal with grain boundary is examined as an application for practical materials.

2 Theory of parallel collective variables-driven hyperdynamics

2.1 Basic theory of original CVHD method

First of all, we give a basic overview of the original CVHD method [12]. Figure 1 shows a schematic image of the concept of CVHD. As in any metadynamics-based method, a CV must be defined. In CVHD, the employed CV is usually based on the bond distortion function [12]. The bond distortion, χ_i is calculated for each bond pair *i* that initially falls inside the cutoff radius as

$$\chi_i = max\left(0, \frac{r_i - r_i^{min}}{r_i^{min}}\right), \tag{1}$$

where r_i and r_i^{min} refer to the length and the starting point of possible reaction events for each bond pair *i*, respectively. Then, the global distortion, *X* is calculated using exponent, *p* as follows

$$X = \left(\sum_i \chi_i^p\right)^{\frac{1}{p}}. \tag{2}$$

In the case of the bond distortion, CV, η is defined as

$$\eta = min\left(\frac{1}{2}\left(1 - \cos\pi\left(\frac{\mathrm{X}}{\chi_{cut}}\right)^2\right), 1\right). \tag{3}$$

In the CVHD method, CV is set to return a value between 0 and 1. The value χ_{cut} is used to ensure that the value of CV is 1 when the bond reaches transition state so that the bias force at the transition state will be zero. After setting the CV, the bias potential in the form of Gaussian functions with width σ and height *W*:

$$\Delta V\left(\eta,t\right)=\sum_{k\tau<t}W(k\tau)\exp\left[-\frac{\left(\eta(t)-\eta\left(k\tau\right)\right)^2}{2\sigma^2}\right], \quad (4)$$

is added at every $k\tau$, where k is integer and τ is the interval. The center of the bias potential is the value of CV at every $k\tau$. If the CV oscillates around a certain value close to zero during the simulation, it means the system is trapped in a metastable state. Therefore, by adding bias to the observed CV step by step, the bias potential will fit the shape of the potential well. This part is the main difference with most other hyperdynamics implementations, which use a static bias that is not easily optimized to be simultaneously suitable for different processes. The height W is modified in order not to add too much bias on one place based on the well-tempered metadynamics scheme [18] as

$$W(k\tau)=W_0\exp\left(-\frac{\Delta V\left(\eta\left(k\tau\right),k\tau\right)}{k_B\Delta T}\right). \quad (5)$$

Here, W_0 is the initial height, k_B is the Boltzmann constant and T is the temperature. ΔT is calculated from a bias factor γ as

$$\gamma=\frac{T+\Delta T}{T}. \quad (6)$$

This bias potential defined in Equation (4) forces the system out of the current free energy basin. After the system leaves this basin and enters a new state, the previously-added bias is removed and the CV is redefined using the bond lengths in the new state as a reference. This means that bias is only added with the goal of escaping the current metastable state, and the bias can be made optimal specifically for this state; a conservative choice of χ_{cut} guarantees that none of this bias is deposited in transition state regions. This is where CVHD differs from conventional metadynamics, in which a bias is continually added to fill up the entire free energy surface along CVs of choice.

The addition of a bias potential accelerates the transition rate in the system. This causes a

discrepancy between the time increment of accelerated MD simulation and that of original (i.e., unbiased) MD simulation. According to transition state theory [6], the acceleration rate, which is the ratio between the time accessed in accelerated MD (τ_{biased}) and original MD (τ_{MD}) can be calculated from the applied bias potential as

$$\frac{\tau_{biased}}{\tau_{MD}} = \left\langle \exp\left[\beta \Delta V(\eta)\right] \right\rangle, \qquad (7)$$

where $\beta = 1/k_b T$, and the brackets < > denote the ensemble average. The accelerated time is also called the hypertime and it is estimated by multiplying the MD time (represented by the accumulated time steps) by this acceleration rate.

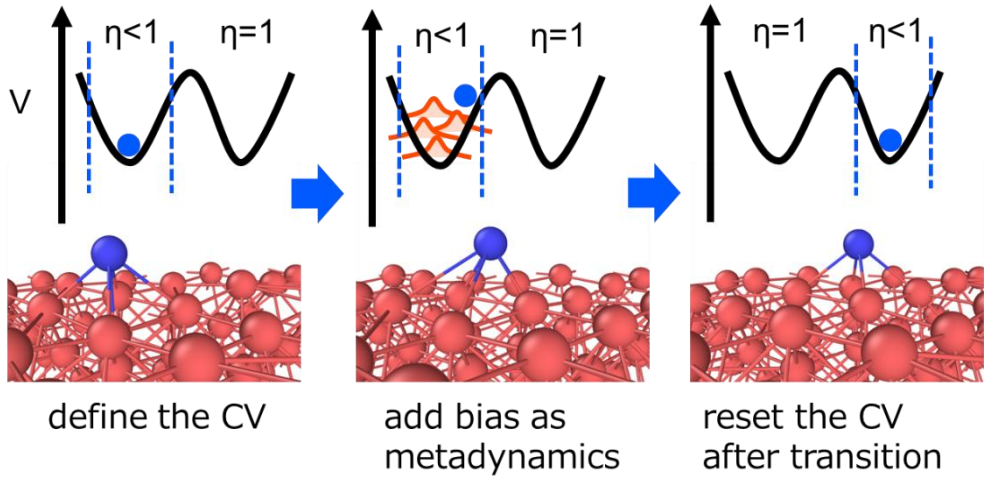

Figure 1. Schematic image of the concept of collective variable-driven hyperdynamics (CVHD).

In this work, diffusion of a carbon atom in a bulk bcc-iron is examined as an example of original CVHD technique. One carbon atom is placed in an interstitial site of bcc-iron crystal consisting of 2000 atoms (i.e., 10 × 10 × 10 unit cells) and a CVHD simulation is run for 10^6 steps, which corresponds to 1000 ps in an original (i.e., no accelerated) MD simulation with a time step of 1 fs. The bond distortion of all C-Fe bonds inside a cutoff distance is calculated and used for the

construction of CV. The cutoff distance is defined as 2.1 Å, which is long enough to capture the C-Fe bond distance (2.03 Å) when a carbon atom is in an octahedron lattice position. $r_{\min}$ is defined as 1.6 Å, which corresponds to the C-Fe bond length when a carbon atom is in a tetrahedral lattice position. χ_{cut} is set to 0.65. Repulsive Gaussians of height w = 0.01 eV and width σ = 0.05 eV were employed as biasing parameters in Equation (4) and the bias potential is added at every 100 fs. A bias factor of 20 is used for the well-tempered metadynamics scheme. All simulations in this study are carried out using the LAMMPS package [19] with the modified version of the PLUMED plugin [12,20]. The embedded atom method (EAM) potential fitted by Lau and coworkers [21] is employed for the interatomic potential of C-Fe binary system. The NPT (the number of atoms, pressure and temperature constant) ensemble is employed using a Nose-Hoover chain thermo- and barostat [22]. Figure 2(a) shows the hypertime evolution during the CVHD simulation at 300 K. The acceleration rate, which corresponds to the slope of the graph, increases as the bias potential is added and decreases again after the transition occurs due to the removal of the bias. Consequently, the shape of the graph becomes staircase-like, that is, steep before the transition and flat after the transition. The average acceleration rate is estimated by dividing the final hypertime by the original time, i.e., the summed integration time. It is confirmed from the figure that the simulation is accelerated with an average acceleration rate of approximately 4.3×10^7 with the CVHD method. In the same manner, we also ran CVHD simulations at 300, 400, and 600 K in addition to unbiased MD simulations at 1000, 1200 and 1400 K for comparison. Figure 2(b) shows the Arrhenius plot of the number of diffusion event as a function of temperature for MD and CVHD simulations. From the slope of fitted lines, activation energies of carbon diffusion are estimated as 0.689 ± 0.015 eV for CVHD and 0.703 ± 0.001 eV for MD without acceleration. Activation energies from two different methods match well, which confirms that CVHD reproduces the dynamics of carbon diffusion correctly.

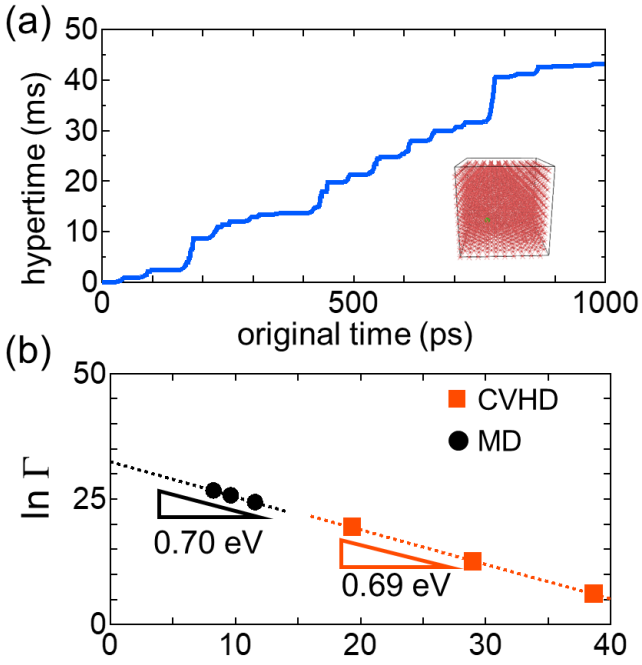

Figure 2. (a) Hypertime evolution during the CVHD simulation of one carbon diffusing in a bcc-iron crystal. The inset shows the initial configuration of the system. (b) Arrhenius plot of the number of diffusion events, Γ as a function of temperature for MD and CVHD simulations. Activation energies of carbon diffusion can be estimated from the slopes of the fitted lines.

2.2 Expansion to parallel CVHD method

Next, let us consider the case where diffusion reactions of two carbon atoms are accelerated simultaneously. The original CVHD method sets one CV and adds a bias to the CV. That is, bonds between carbon and surrounded iron atoms are taken into consideration as one global distortion as described in Equation (2). Therefore, all bonds between each carbon atom and their surrounding iron atoms are added into same global distortion (see Figure 3 (a)). Figure 3(b) shows the hypertime evolution during the simulation of the diffusion of two carbon atoms in bcc-iron crystal by CVHD, using the same biasing parameters. The average acceleration rate for the diffusion of two carbon atoms is about 1.7×10^7, which is just half of the case of the

acceleration of the diffusion of one carbon atom. It means that the acceleration rate decreases as the number of diffusing carbon atoms to be accelerated increases, which is a problem of the original CVHD that we wish to improve. The problem originates from using a single CV in the original CVHD algorithm. As a consequence, any diffusion event in the system will trigger a reset of the bias on all atoms, reducing the average bias potential applied on the system. Thus, the acceleration efficiency drastically decreases as the number of atoms increases.

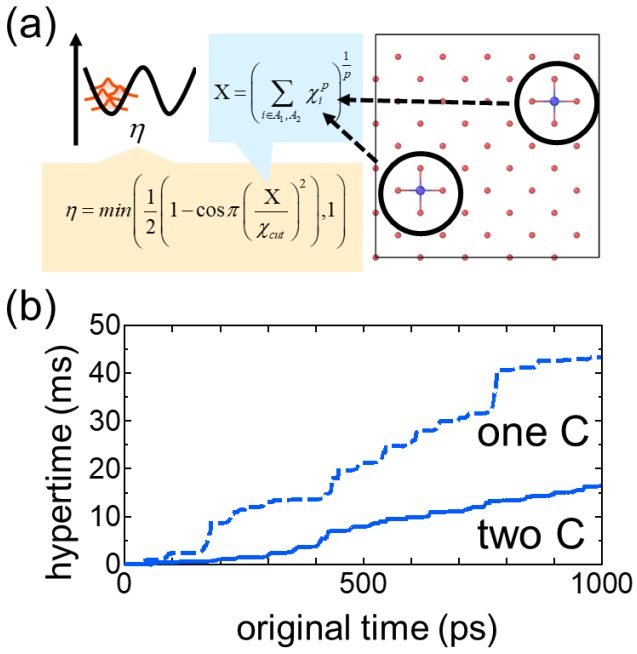

Figure 3. (a) Schematic image of the CV set for the acceleration of diffusion of two carbon atoms in bcc-iron crystal using the original CVHD method. (b) Hypertime evolution during the simulation of diffusion of two carbon atoms using the original CVHD method (solid line). For comparison, that for one carbon atom in Figure 2(a) is plotted as a dashed line.

Here, a new method to run CVHD in parallel is developed to overcome this problem. Specifically, CV η_j is set for each target atom and bias potential is added to each CV separately.

Equations (2) and (3) are modified as

$$\mathrm{X}_j = \left(\sum_{i \in A_j} \chi_i^p \right)^{\frac{1}{p}}, \tag{8}$$

$$\eta_j = min\left(\frac{1}{2}\left(1 - \cos \pi \left(\frac{\mathrm{X}}{\chi_{cut}} \right)^2 \right), 1 \right), \tag{9}$$

where A_j represents a list of bond pairs for each CV η_j. Then, the bias is added to each group of target bonds A_j separately as

$$\Delta V_j(\eta, t) = \sum_{k\tau < t} W(k\tau) \exp\left[-\frac{\left(\eta_j(t) - \eta_j(k\tau)\right)^2}{2\sigma^2} \right]. \tag{10}$$

This is the same expression as in equation (4), with the difference that each CV η_j now has its own bias potential. Practically, such an approach corresponds to performing several independent CVHD simulations in parallel, each in their own part of the system. The schematic image of the concept of this method is shown in Figure 4(a).

Using above definition, a parallel CVHD calculation is performed on a same system as shown in Figure 3(b), but with the bonds around each carbon atom *j* put in a separate to-be-biased group A_j. Figure 4(b) shows hypertime evolution during the simulation of diffusion of two carbon atoms in bcc-iron crystal by the parallel CVHD technique. The average acceleration rates for the two carbon atoms are 3.5×10^7 and 2.7×10^7, respectively. The acceleration efficiency of each carbon atom does not decrease drastically when the CVHD is run in parallel; the small observed decrease can be caused by different diffusion paths. In order to confirm this as well as to examine the effect of the number of target atoms on the acceleration efficiency, further calculations are performed in systems with one, two, four and eight carbon atoms. Figure 5 shows the acceleration rate as a function of the number of accelerated carbon atoms in standard (one CV) and parallel (multiple CVs) CVHD simulations. Five replicate calculations are performed for each condition

to gather statistics. It can be seen that the acceleration rate remains almost constant even with increasing the number of carbon atoms in the case of parallel CVHD simulations, whereas the acceleration rate decreases drastically with increasing number of carbon atoms in the standard CVHD simulation with one CV. This shows that the parallel CVHD technique accelerates the multiple target atoms quite successfully.

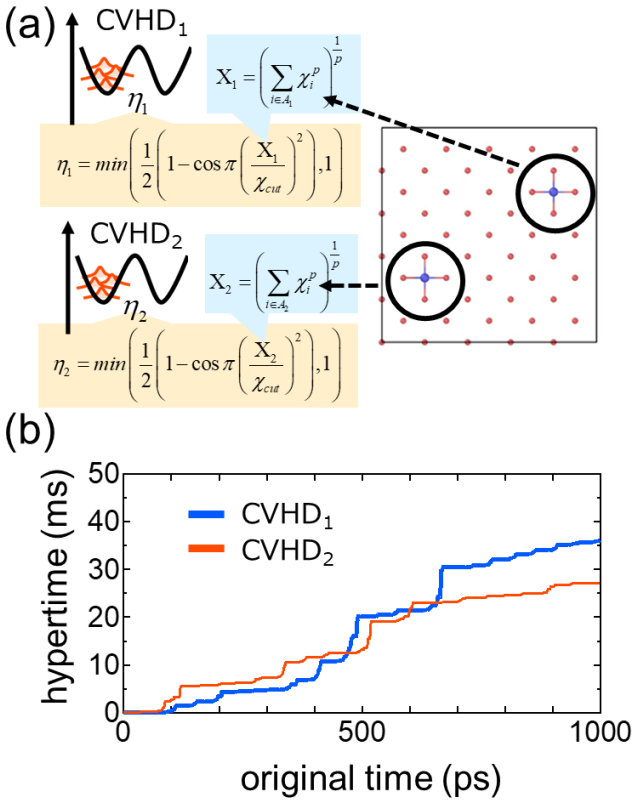

Figure 4. (a) Schematic image of CVs set for the acceleration of diffusion of two carbon atoms using parallel CVHD method. (b) Hypertime evolution for each atom during the simulation of diffusion of two carbon atoms in bcc-iron crystal by the parallel CVHD method.

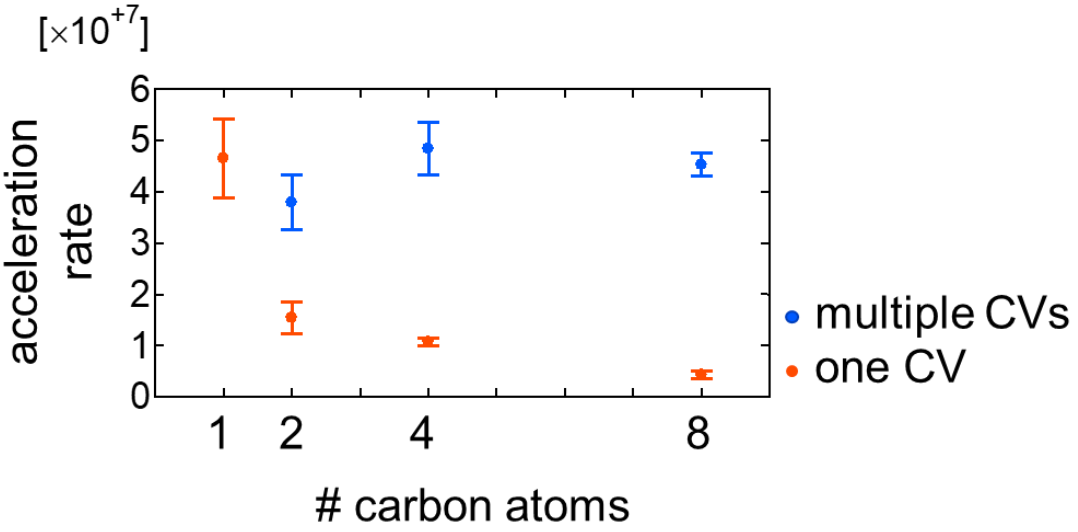

Figure 5. Acceleration rate as a function of the number of accelerated carbon atoms in original (one CV) and parallel (multiple CVs) CVHD simulations. The average rate obtained from five replicate calculations for each condition is plotted with error bars showing the standard deviation.

2.3 Rate control of parallel CVHD simulation

Although all atoms are successfully accelerated by the parallel CVHD simulation, the acceleration rate of each atom fluctuates since each atom is accelerated independently by a separate CV. In fact, the acceleration rate of two atoms in Figure 4(b) is 3.5×10^{7} and 2.7×10^{7}, respectively. This means that the physical time scale accessed in different parts of the system is not the same.

In this section, methodology to control the acceleration rate among all of target atoms is discussed. There is a method using a boostostat [8] to control the acceleration rate in the local hyperdynamics method, in which a static bias is employed. However, it is not straightforward to employ this method into the parallel CVHD method since the applied form of the bias potential is not known *a priori* because it is based on metadynamics. Therefore, we propose a new strategy

for the rate control in the parallel CVHD technique as follows. The rate control process consists of two operations:

(i) Stop adding a new bias potential

(ii) Remove the last added bias potential

by which acceleration rate is suppressed to the pre-defined target acceleration rate.

We explain a practical procedure of the rate controlled parallel CVHD technique using an example of the schematic image in Figure 6(a). In the schematic image, the estimated hypertime for the first 3 bias addition steps is lower than the target hypertime and it becomes higher at the 4th step. In the all of the previous CVHD simulations of the previous sections, new hills are added until the expected reaction happens, without having specified a target hypertime (the dashed line in Figure 6(a)). On the other hand, no new bias potential is added in the rate-controlled- parallel CVHD method here once the estimated hypertime becomes higher than the target hypertime (operation (i)). However, it is not enough to stop adding a new bias potential since the acceleration rate (i.e., the slope of hypertime as a function of original time) is the same as that of previous step only by the operation (i) (the dotted line in Figure 6(a)), which means that the hypertime will keep increasing. Therefore, the last-added bias (the bias 3 in the schematic image) is also removed, so that the acceleration rate is reduced until its value after step 2. This process is repeated until the current hypertime becomes lower than the target one. In the schematic image in Figure 6(a), above processes are repeated until the 5th step and a new bias is added at the 6th step again, where the estimated hypertime at the 6th step becomes lower than the target one. By applying this control continuously, the acceleration rate remains close to the pre-defined target acceleration rate correctly.

Note that the acceleration rate of certain reaction along a CV η_a is correct only when no bias associated with any other CV η_b affects the target reaction because the acceleration rate is

calculated from the bias added on η_a. In the specific bond-based CVHD implementation used here, this loosely speaking means that CVs should not share any bonds: In the applications discussed in this paper, each CV is centered on one carbon atom, which avoids this issue by construction. In more strict terms, processes biased by different CVs should occur beyond the cutoff distance of the interatomic potential.

Using this methodology, a rate-controlled parallel CVHD calculation is performed on a same system as shown in Figure 4 (b) (i.e., two carbon atoms in bcc-iron crystal). Calculations with acceleration rate of 2.0×10^7 and $1.0\times10^7$are performed. Figure 6(b) shows the hypertime evolution during the simulation of two diffusing carbon atoms in bcc-iron crystal by rate-controlled parallel CVHD technique. The hypertime evolution of the two carbon atoms is the same and matches the target acceleration rate for both acceleration rates. Thus, we successfully developed the rate-controlled parallel CVHD method.

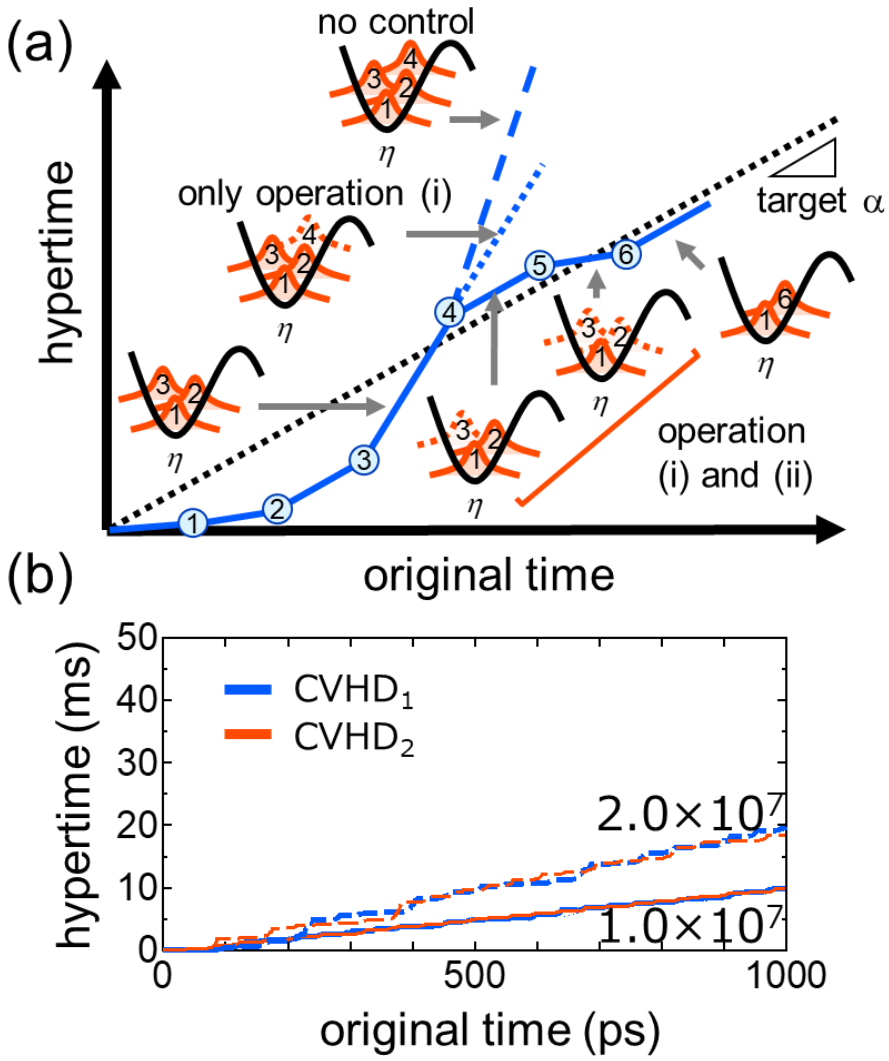

Figure 6. (a) Schematic image of the rate-controlled parallel CVHD technique. (b) Hypertime evolution of both atoms during the simulation of diffusion of two carbon atoms in bcc-iron crystal by the rate-controlled parallel CVHD technique with imposed acceleration rate of 1.0×10^7 and 2.0×10^7.

We note that recently, Fu and Pfaendtner also proposed a biasing strategy based on a parallel bias potential [23]. However, the focus of their approach is the exploration of reaction networks involving small molecules, and no explicit time scale recovery or system evolution is obtained. Moreover, by using the so-called social permutation invariant (SPRINT) coordinates [24] as CVs, the method is likely limited to fairly small systems because it requires the explicit

diagonalization of the contact matrix in the system. The two approaches therefore serve different purposes, while both being useful parts of the computational toolbox.

3. Application

The rate-controlled parallel CVHD method is now applied to the diffusion of multiple carbon atoms in bcc-iron bicrystal with a grain boundary as an application for practical materials. Actually, carbon diffusion in iron and steel are quite important for the practical process of steel making since carbon diffusion is one of the dominant factors for the phase transformation via heat treatment processes [25]. Also, it is well known that carbon segregation strongly affects the mechanical properties of the final products [26]. Here, carbon diffusion in a bcc-iron bicrystal with Σ3<110>(112) (i.e. twin boundary) and Σ3<110>(111) symmetric tilt grain boundary (GB) [26-28] is investigated. Figure 7 shows the initial configurations of bicrystal systems. The bicrystals with (112)GB and (111)GB consist of 27072 and 27264 iron atoms, respectively. 27 carbon atoms are randomly located in interstitial sites of the bcc crystals, which corresponds to around 0.1 atomic%. Rate controlled parallel CVHD simulations are run for the two systems during 5×10^{6} steps at 300 K with an imposed acceleration rate of 2.0×10^{7}. It corresponds to 100 ms of the hypertime, which is much longer than the time scale of a conventional MD simulation. The other calculation conditions are the same as for the simulations performed in Section 2.

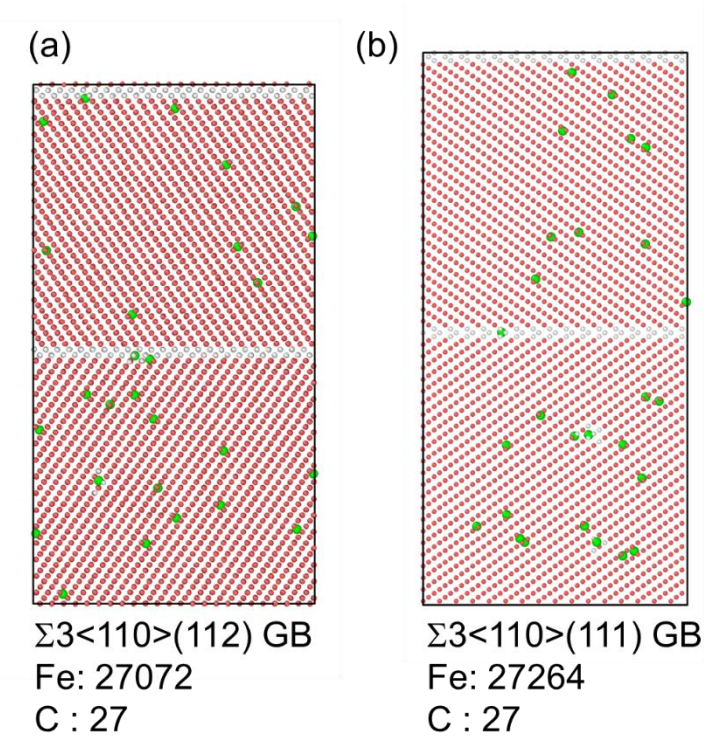

Figure 7. Initial configuration of bcc-iron bicrystal with (a) Σ3<110>(112) and (b) Σ<110>(111) symmetric tilt grain boundary (GB). Red, green and white spheres represent iron atoms in the bulk region, carbon atoms and iron atoms at the grain boundary, respectively.

Figure 8 shows trajectories of all carbon atoms during the simulation projected onto a two-dimensional plane. Iron atoms belonging to the grain boundary or other types of defects at the final calculation step are shown in light-blue. Iron atoms with bulk bcc configuration are not shown for clarity. Each carbon atom does not get close to another, which makes it possible to treat each diffusion path independently. It is confirmed that the (111)GB moves easily during the simulation due to the high grain boundary energy, whereas the (112)GB with extraordinary small grain boundary energy [27], keeps its structure at the initial position throughout the simulation. This tendency agrees with the previous report of grain boundary properties at high temperature [28]. In any case, carbon atoms in the bulk region diffuse randomly during the CVHD simulation,

whereas carbon atoms reaching the grain boundary are trapped and stay around the trapped position. This is regarded as grain boundary segregation of carbon, which is a typical phenomenon observed in the steelmaking process [29]. This means that energy barriers of carbon diffusion in the bulk region and at the grain boundary are different. Figure 9 shows the hypertime evolution during the simulation for two representative carbon atoms in each system: one in the bulk region and the other at the grain boundary for both systems with (112)GB and (111)GB, respectively. The acceleration rate basically follows the target rate for both atoms in the bulk and at the grain boundary. It means that multiple events with different event frequencies are accelerated simultaneously at a target rate by the rate-controlled parallel CVHD method proposed in this study. Therefore, the overall time evolution of the system in the accelerated simulation will be fully equivalent to very long unbiased MD simulations. Note that in this simulation only carbon atom diffusion is accelerated, and GB migration is not accelerated. Therefore, the effect of GB migration, which occurs at a long timescale compared to original MD, cannot be discussed. However, the static effect of the GB on the motion of the carbon atoms will be captured in the simulation.

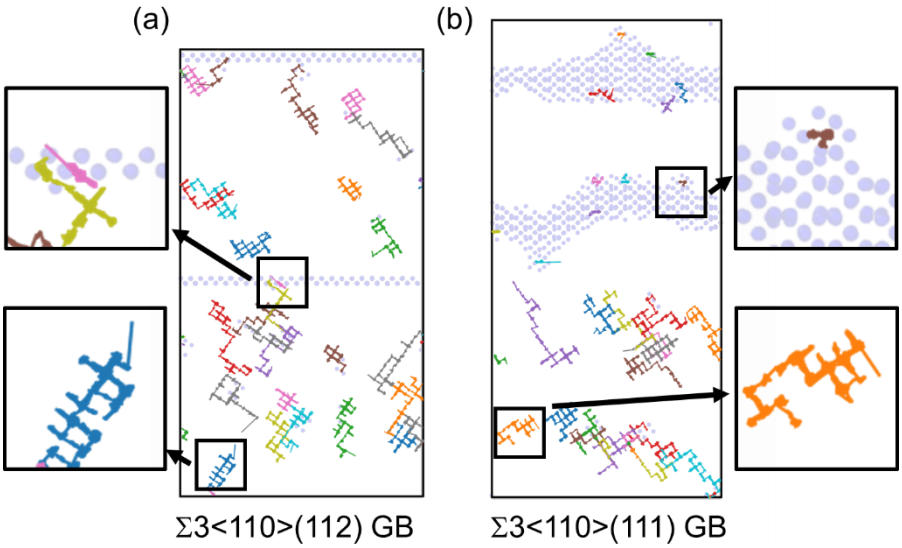

Figure 8. Trajectory of all carbon atoms during the simulation projected onto the two-dimensional plane for the system with (a) Σ3<110>(112) and (b) Σ3<110>(111) symmetric tilt grain boundary (GB). Light-blue atoms represent iron atoms with disordered structures (i.e., grain boundary, point defect and so on) defined by common neighbor analysis for the snapshot of the final step of the simulation. The other iron atoms are not shown for the clarity of the image. Insets show enlarged views of trajectories for representative atoms in the bulk and at the grain boundaries in bicrystal systems.

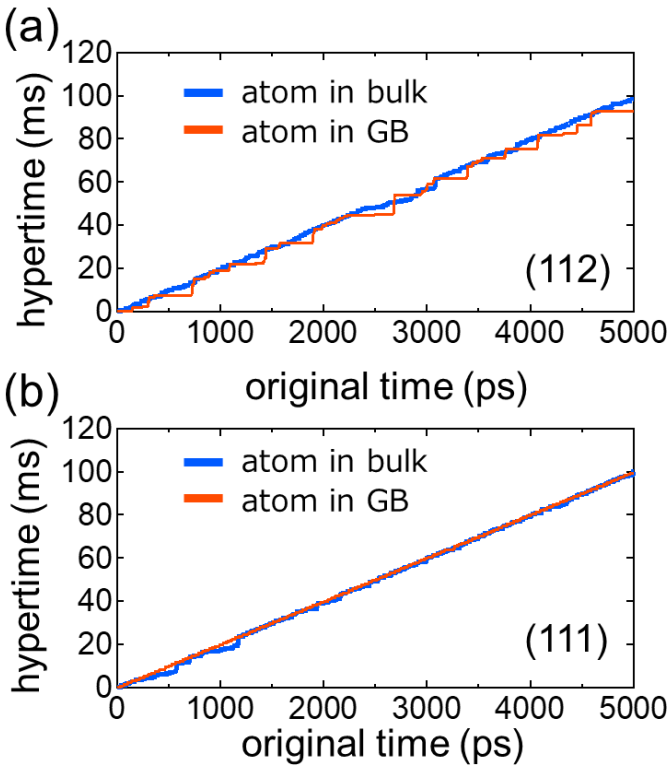

Figure 9. Hypertime evolution during the simulation of diffusion of 27 carbon atoms in bcc-iron bicrystal with (a) Σ3<110>(112) and (b) Σ3<110>(111) symmetric tilt grain boundary by rate-controlled parallel CVHD simulation.

4. Conclusion

In this study, rate-controlled acceleration method for the MD simulation is developed based on the original CVHD method with one CV. Since the acceleration rate decreases as the number of target atoms to be accelerated increases in the original CVHD method, a new method to run CVHD in parallel is proposed, in which multiple CVs are biased independently. The acceleration rate in each subset of the system, described by its own CV, can be controlled and kept syncronized, which is the merit of the proposed model. Using this methodology, diffusion of multiple carbon atoms in bcc-iron bicrystal with grain boundary was examined. Carbon atoms reaching at the grain boundary are trapped and keep staying around the trapped position, whereas

carbon atoms in the bulk region diffuse randomly. We emphasize that the parallel CVHD technique proposed in this study can consistently and equally accelerate processes in different parts of the system with different event frequencies simultaneously at a target rate. Moreover, parallel CVHD can correctly simulate the dynamical system evolution in materials over a millisecond time scale which is impossible to achieve by conventional MD simulation. The parallel CVHD technique developed in this study is expected to be applicable to many practical diffusion-limited phenomena such as precipitation, age hardening and diffusion bonding.

CRediT authorship contribution statement

Satoru Fukuhara: Conceptualization, Data curation, Formal analysis, Investigation, Methodology, Validation, Visualization, Writing - original draft, Writing - review & editing. **Kristof M. Bal**: Conceptualization, Methodology, Validation, Visualization, Writing - review & editing. **Erik C. Neyts**: Conceptualization, Methodology, Validation, Resources, Supervision, Writing - review & editing. **Yasushi Shibuta**: Conceptualization, Formal analysis, Funding acquisition, Investigation, Methodology, Resources, Supervision, Validation, Visualization, Writing – original draft, Writing - review & editing.

Acknowledgements

This work was supported by Grant-in-Aid for Scientific Research (B) (No.19H02415) and Grant-in-Aid for JSPS Research Fellow (No.18J22727) from Japan Society for the Promotion of Science (JSPS), Japan. S.F. was supported by JSPS through the Program for Leading Graduate Schools (MERIT).

Data availability

The data required to reproduce these findings are available from the corresponding authors upon reasonable request.

References

[1] Y. Shibuta, M. Ohno, T. Takaki, Advent of cross-scale modeling: High-performance computing of solidification and grain growth, Adv. Theory Simulations. 1 (2018) 1800065.

[2] Y. Shibuta, S. Sakane, E. Miyoshi, S. Okita, T. Takaki, M. Ohno, Heterogeneity in homogeneous nucleation from billion-atom molecular dynamics simulation of solidification of pure metal, Nat. Commun. 8 (2017) 1–8.

[3] Y. Shibuta, S. Sakane, E. Miyoshi, T. Takaki, M. Ohno, Micrometer-scale molecular dynamics simulation of microstructure formation linked with multi-phase-field simulation in same space scale, Model. Simul. Mater. Sci. Eng. 27 (2019) 054002.

[4] E. Miyoshi, T. Takaki, Y. Shibuta, M. Ohno, Bridging molecular dynamics and phase-field methods for grain growth prediction, Comp. Mater. Sci., 152 (2018) 118–124.

[5] G.G. Tibbetts, Diffusivity of carbon in iron and steels at high temperatures, J. Appl. Phys. 51 (1980) 4813–4816.

[6] A.F. Voter, Hyperdynamics: Accelerated Molecular Dynamics of Infrequent Events, Phys. Rev. let. 78 (1997) 3908–3911.

[7] Y. Shim, J.G. Amar, B.P. Uberuaga, A.F. Voter, Reaching extended length scales and time scales in atomistic simulations via spatially parallel temperature-accelerated dynamics, Phys. Rev. B 76 (2007) 205439.

[8] S.Y. Kim, D. Perez, A.F. Voter, Local hyperdynamics, J. Chem. Phys. 139 (2013) 144110.

[9] A. Laio, M. Parrinello, Escaping free-energy minima, Proc. Natl. Acad. Sci. U. S. A. 99 (2002) 12562–12566.

[10] A. Ishii, S. Ogata, H. Kimizuka, J. Li, Adaptive-boost molecular dynamics simulation of carbon diffusion in iron, Phy. Rev B. 85 (2012) 064303.

[11] J. Li, S. Sarkar, W.T. Cox, T.J. Lenosky, E. Bitzek, Y. Wang, Diffusive molecular dynamics and its application to nanoindentation and sintering, Phys. Rev. B 84 (2011) 054103.

[12] K.M. Bal, E.C. Neyts, Merging Metadynamics into Hyperdynamics: Accelerated Molecular Simulations Reaching Time Scales from Microseconds to Seconds, J. Chem. Theory Comput. 11 (2015) 4545–4554.

[13] K.M. Bal, E.C. Neyts, Direct observation of realistic-temperature fuel combustion mechanisms in atomistic simulations, Chem. Sci. 7 (2016) 5280–5286.

[14] K. Ganeshan, M.J. Hossain, A.C.T. van Duin, Multiply accelerated ReaxFF molecular dynamics: coupling parallel replica dynamics with collective variable hyper dynamics, Mol. Simul. 45 (2019) 1265–1272.

[15] D.U.B. Aussems, K.M. Bal, T.W. Morgan, M.C.M. Van De Sanden, E.C. Neyts, Atomistic simulations of graphite etching at realistic time scales, Chem. Sci. 8 (2017) 7160–7168.

[16] D.U.B. Aussems, K.M. Bal, T.W. Morgan, M.C.M. van de Sanden, E.C. Neyts, Mechanisms of elementary hydrogen ion-surface interactions during multilayer graphene etching at high surface temperature as a function of flux, Carbon 137 (2018) 527–532.

[17] K.M. Bal, S. Huygh, A. Bogaerts, E.C. Neyts, Effect of plasma-induced surface charging on catalytic processes: Application to CO2 activation, Plasma Sources Sci. Technol. 27 (2018) 024001.

[18] A. Barducci, G. Bussi, M. Parrinello, Well-tempered metadynamics: A smoothly converging and tunable free-energy method, Phys. Rev. Lett. 100 (2008) 020603.

[19] S. Plimpton, Fast parallel algorithms for short-range molecular dynamics, J. Comput. Phys. 117 (1995) 1–19.

[20] G.A. Tribello, M. Bonomi, D. Branduardi, C. Camilloni, G. Bussi, PLUMED 2: New feathers for an old bird, Comput. Phys. Commun. 185 (2014) 604–613.

[21] T. T. Lau, C. J. Först, X. Lin, J. D. Gale, S. Yip, K. J. VanVliet, Many-body potential for point defect clusters in Fe-C alloys, Phys. Rev. Lett. 98 (2007) 215501.

[22] G.J. Martyna, D.J. Tobias, M.L. Klein, Constant pressure molecular dynamics algorithms, J. Chem. Phys. 101 (1994) 4177–4189.

[23] C.D. Fu, J. Pfaendtner, Lifting the curse of dimensionality on enhanced sampling of reaction networks with parallel bias metadynamics, J. Chem. Theory Comput. 14 (2018) 2516–2525.

[24] F. Pietrucci, W. Andreoni, Graph theory meets ab initio molecular dynamics: Atomic structures and transformations at the nanoscale, Phys. Rev. Lett. 107 (2011) 085504.

[25] R.W. Balluffi, S.M. Allen, W.C. Carter, Kinetics of materials, Wiley-Interscience, Hoboken, 2005.

[26] A.P. Sutton, R.W. Balluffi, Interfaces in crystalline materials, Oxford University Press, Oxford 1995.

[27] Y. Shibuta, S. Takamoto, T. Suzuki, A molecular dynamics study of the energy and structure of the symmetric tilt boundary of iron, ISIJ Int. 48 (2008) 1582–1591.

[28] Y. Shibuta, S. Takamoto, T. Suzuki, Dependence of the grain boundary energy on the alloy composition in the bcc iron-chromium alloy: a molecular dynamics study, Comp. Mater. Sci. 44 (2009) 1025–1029.

[29] J. Takahashi, M. Sugiyama, N. Maruyama, Quantitative observation of grain boundary carbon segregation in bake-hardening steels, Nippon Steel Tech. Report, 91 (2005) 28–33.